



# Fermi National Accelerator Laboratory

FERMILAB-Conf-99/117-E

CDF

## New Phenomena Searches at the Tevatron

A. Nomerotski

For the CDF Collaboration

*University of Florida*

*Fermi National Accelerator Laboratory*

*P.O. Box 500, Batavia, Illinois 60510*

May 1999

Published Proceedings of the *34th Rencontres de Moriond: Electroweak Interactions and Unified Theories*, Les Arcs, France, March 13-20, 1999

## **Disclaimer**

*This report was prepared as an account of work sponsored by an agency of the United States Government. Neither the United States Government nor any agency thereof, nor any of their employees, makes any warranty, expressed or implied, or assumes any legal liability or responsibility for the accuracy, completeness, or usefulness of any information, apparatus, product, or process disclosed, or represents that its use would not infringe privately owned rights. Reference herein to any specific commercial product, process, or service by trade name, trademark, manufacturer, or otherwise, does not necessarily constitute or imply its endorsement, recommendation, or favoring by the United States Government or any agency thereof. The views and opinions of authors expressed herein do not necessarily state or reflect those of the United States Government or any agency thereof.*

## **Distribution**

*Approved for public release; further dissemination unlimited.*

## **Copyright Notification**

*This manuscript has been authored by Universities Research Association, Inc. under contract No. DE-AC02-76CHO3000 with the U.S. Department of Energy. The United States Government and the publisher, by accepting the article for publication, acknowledges that the United States Government retains a nonexclusive, paid-up, irrevocable, worldwide license to publish or reproduce the published form of this manuscript, or allow others to do so, for United States Government Purposes.*

# New phenomena searches at the Tevatron

Andrei Nomerotski  
*University of Florida*

## **Abstract**

Proceedings of EWK Rencontres de Moriond, Les Arc, March 13-20 1999.

## NEW PHENOMENA SEARCHES AT TEVATRON

ANDREI NOMEROTSKI

*University of Florida, Gainesville, FL 32611 USA*



We present here recent searches at the Tevatron for new phenomena. The superlight gravitino, scalar top and scalar bottom quarks searches are described in the framework of the supersymmetric models. We also discuss the new Tevatron limits on the second and third generations leptoquark masses.

## 1 Tevatron and its detectors

The Tevatron is the world largest  $p\bar{p}$  collider at Fermilab with the 1.8 TeV center of mass energy. During Run I in 1992-1996 the DØ<sup>1</sup> and CDF<sup>2</sup> detectors accumulated over 100 pb<sup>-1</sup> of data per experiment. The high energy of collisions and the large accumulated luminosity make new phenomena searches with these detectors especially interesting.

## 2 SUSY searches

The Standard Model (SM) successfully describes the existing experimental information. However, it has problems from the theoretical point of view. The SM Lagrangian contains terms that are divergent unless exceptionally fine tuning takes place<sup>3</sup>. Supersymmetric (SUSY) model<sup>4</sup> introduces a new type of symmetry, between bosons and fermions. It assigns to each of SM particle a superpartner (or a sparticle) with a spin different by 1/2 which solves the problem of fine-tuning. The price for this is a large number of parameters which leads to a variety of possible superpartners mass spectra.

In all SUSY searches described here it is assumed that R-parity is conserved (i.e. decay products of a supersymmetric particle include at least one supersymmetric particle). In this case the Lightest Supersymmetric Particle (LSP) must be stable, and neutral for the cosmological reasons. From the experimental point of view, a stable neutral LSP escapes the detector undetected giving the classic SUSY signature at the hadron colliders : missing transverse energy ( $\cancel{E}_T$ ). Another important consequence of the R-parity conservation is the pair production of the supersymmetric particles at the Tevatron.

### 2.1 CDF superlight gravitino search

Gravitino ( $\tilde{G}$ ) is the spin 3/2 superpartner of graviton.  $\tilde{G}$  is often the LSP in the Gauge Mediated SUSY Breaking (GMSB) class of SUSY models<sup>5</sup>. In a scenario when the gravitino is very light and all other supersymmetric particles are above the production threshold, the pair  $\tilde{G}\tilde{G}$  production can still be observed. Of course, the leading order process is invisible but the QCD Initial State Radiation (ISR) makes it observable resulting in a monojet signature. Processes:  $q\bar{q} \rightarrow \tilde{G}\tilde{G}g, qg \rightarrow \tilde{G}\tilde{G}q, gg \rightarrow \tilde{G}\tilde{G}g$  will lead to a topology with a high  $E_T$  jet balanced with large  $\cancel{E}_T$ <sup>6</sup>. When all other SUSY particles are heavy, the production cross section depends only on the SUSY breaking scale  $\sqrt{F}$  as  $\sigma \propto F^{-4}$ .  $F$  can be expressed via the gravitino mass and Plank mass as follows :  $F = \sqrt{3}m_{\tilde{G}}M_P$ . Note that no assumption is made on the sparticles spectrum. The cross section depends on partons energy cutoff and, hence, on the analysis  $E_T$  and  $\cancel{E}_T$  cuts.

CDF performed a search for the gravitino pairs accompanied by a jet in 89 pb<sup>-1</sup> of Run Ib data using the  $\cancel{E}_T$  sample with the  $\cancel{E}_T$  trigger threshold of 35 GeV. After the initial cleanup at least one jet with  $E_T > 80$  GeV and no leptons were required. The left plot in Figure 1 shows the distribution in  $\Delta\phi$  between  $\cancel{E}_T$  and the closest jet.

The instrumental background, coming from the energy mismeasurement for the back-to-back QCD di-jet events, can be effectively eliminated by the  $\Delta\phi > 90^\circ$  cut. The  $\cancel{E}_T$  distribution after  $\Delta\phi$  cut is shown in the right plot in Figure 1. The remaining SM backgrounds are further suppressed by the  $\cancel{E}_T > 200$  GeV cut.

After all cuts 5 events were observed in the data which agrees with  $10.1 \pm 3.4$  expected from the SM backgrounds, with the largest background from the Z ( $\rightarrow \nu\bar{\nu}$ ) + jets production. The gravitino signal acceptance is equal to 79%. The largest systematic uncertainty of 50% in this analysis is conservatively assigned to ISR and work is in progress to decrease this systematic. With this information CDF excludes the SUSY breaking scale  $\sqrt{F} \leq 203$  GeV and  $m_{\tilde{G}} \leq 1.0 \cdot 10^{-5}$  eV/c<sup>2</sup> at 95% CL.

### 2.2 CDF and DØ 3<sup>rd</sup> generation scalar quarks searches

In SUSY the SM quark helicity states  $q_L$  and  $q_R$  acquire scalar partners  $\tilde{q}_L$  and  $\tilde{q}_R$ . Most models predict that the masses of the first two generations of scalar quarks are approximately degenerate.

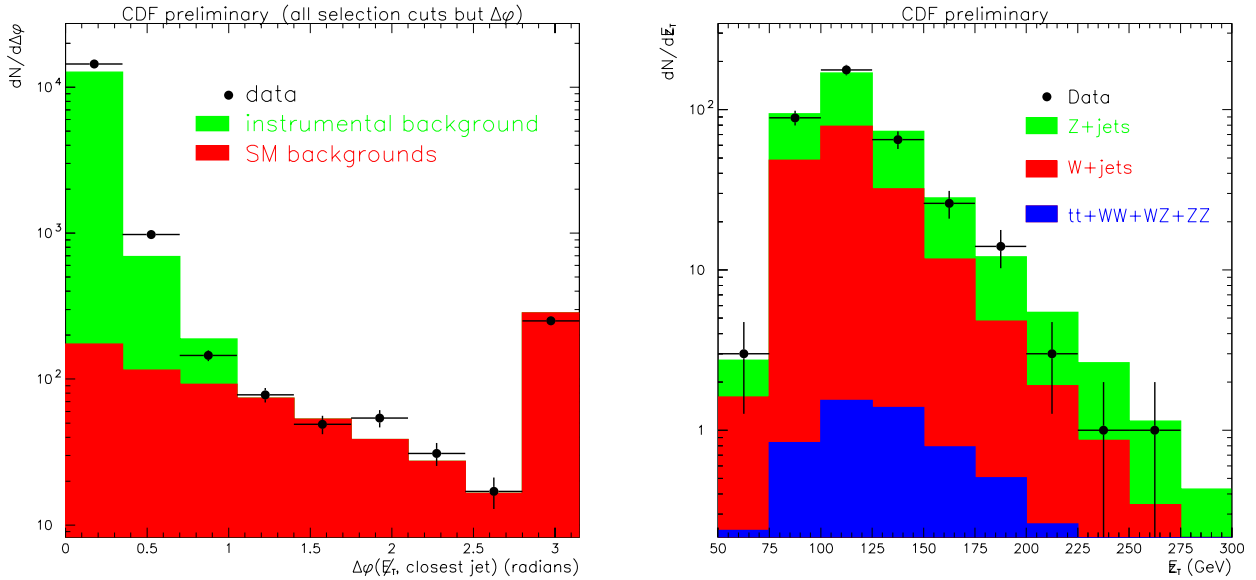


Figure 1: Left plot: Distribution on  $\Delta\phi$  between  $\cancel{E}_T$  and the closest jet. Right plot: Distribution on  $\cancel{E}_T$  after  $\Delta\phi$  cut. The final cut is at  $\cancel{E}_T = 200$  GeV.

The scalar top quark ( $\tilde{t}$ ) mass, however, may be lower than that of the other scalar quarks due to a substantial Yukawa coupling resulting from the large top quark mass. In addition, mixing between  $\tilde{t}_L$  and  $\tilde{t}_R$  can cause a large splitting between the mass eigenstates<sup>7</sup>. This can lead to a scalar top quark which is not only the lightest scalar quark but also lighter than the top quark.

The bottom quark mass is much smaller than the top quark mass, so the effect of the Yukawa coupling on the scalar bottom quark ( $\tilde{b}$ ) mass is small. However, in some regions of supersymmetric parameter space a large mixing between  $\tilde{b}_L$  and  $\tilde{b}_R$  can still occur leading to a significant splitting between mass eigenstates.

At the Tevatron, the third generation scalar quarks are produced in pairs via  $gg$  and  $q\bar{q}$  fusion. For the scalar top quark search CDF considered the  $\tilde{t}_1 \rightarrow c\tilde{\chi}_1^0$  decay mode. In the absence of flavor changing neutral currents (FCNC) this decay proceeds via a one-loop diagram and will become dominant when the tree-level decay  $\tilde{t}_1 \rightarrow b\tilde{\chi}_1^+$  is kinematically forbidden. For the scalar bottom quark search the  $\tilde{b}_1 \rightarrow b\tilde{\chi}_1^0$  decay mode was considered. Since this is a tree-level decay it dominates over most of the parameter space if  $\tilde{\chi}_2^0$  is heavier than  $\tilde{b}_1$ .

The signature of third generation scalar quark production and decay considered here is 2 acolinear heavy flavor jets, significant missing transverse energy ( $\cancel{E}_T$ ), and no leptons in the final state.  $\tilde{t}\tilde{t}$  production will result in two charm jets, while  $\tilde{b}\tilde{b}$  in two bottom jets.

The same  $\cancel{E}_T$  dataset was used by CDF as for the gravitino search discussed above.

Events with 2 or 3 jets with  $E_T \geq 15\text{GeV}$  and  $|\eta| \leq 2$  were selected. The  $\cancel{E}_T$  cut was increased to 40 GeV beyond the trigger threshold of 35 GeV. To reduce the contribution from processes where missing energy comes from jet energy mismeasurement CDF required that the  $\cancel{E}_T$  direction is neither parallel to any jet nor anti-parallel to the leading  $E_T$  jet :  $\min \Delta\phi(\cancel{E}_T, j) > 45^\circ$ ,  $\Delta\phi(\cancel{E}_T, j_1) < 165^\circ$ , and  $45^\circ < \Delta\phi(j_1, j_2) < 165^\circ$ , where the jet indices are ordered by decreasing  $E_T$ . Events with one or more identified electrons (muons) with  $E_T(P_T) > 10$  GeV(GeV/c) were rejected.

The dominant source of background for this analysis is the production of  $W$ +jets, where the  $W$  decays to a neutrino (leading to missing energy) and an electron or muon that is not identified, or a  $\tau$  which decays hadronically.

The lifetime information is used to tag heavy flavor jets. For each track the probability that the track comes from the primary vertex is determined taking into account the impact parameter resolution. By construction, the distribution of track probability is flat for tracks originating from the

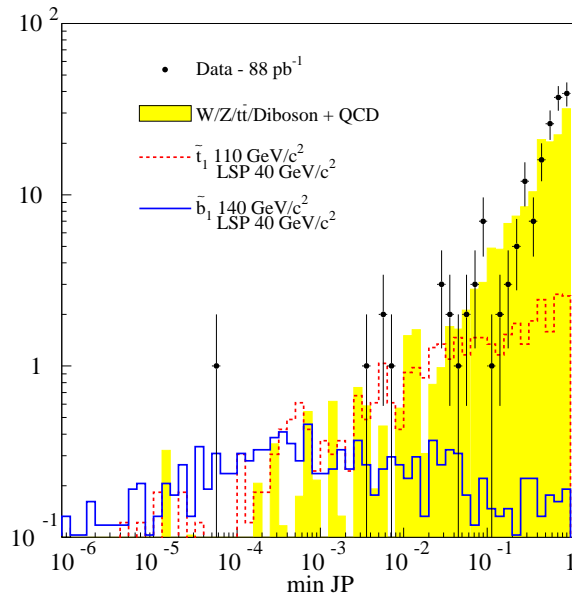


Figure 2: The distribution of  $\min(\text{JP})$  - the lowest value of JP for all taggable jets in an event. Points are data, the shaded histogram is the sum of the predicted backgrounds, the solid line is the predicted signal for scalar top and the dashed line is the predicted signal for scalar bottom. The background and signal are normalized to  $88 \text{ pb}^{-1}$ .

primary vertex. For tracks from a secondary vertex, this distribution peaks near 0. The combination of track probabilities for tracks associated to a jet is called *jet probability*. Jet probability is flat for a primary jet data sample. For bottom and charm jets, jet probability peaks near 0.

The distribution of minimum jet probability of the jets is shown in Figure 2. To select charm jets for the scalar top search analysis CDF required that at least one jet has a probability of less than 0.05. This cut, selected to optimize the sensitivity, rejects about 97% of the background while its efficiency for the signal is about 25%. For bottom jet selection in the scalar bottom search, the signal significance is optimized by requiring that at least one jet has a probability of less than 0.01.

In the scalar top analysis 11 events were selected in data, which is consistent with  $14.5 \pm 4.2$  events expected from standard model processes. The total systematic uncertainty is equal to 36% with the largest contribution from the QCD initial and final state radiation.

The null result in the scalar top search is interpreted as an excluded region in the  $m_{\tilde{t}_1} - m_{\tilde{\chi}_1^0}$  parameter space as shown in the left plot of Figure 3. The maximum  $m_{\tilde{t}_1}$  excluded is  $119 \text{ GeV}/c^2$  for  $m_{\tilde{\chi}_1^0} = 40 \text{ GeV}/c^2$ . The reach in  $m_{\tilde{t}_1}$  is limited by the accumulated luminosity, while the gap between the kinematic limit and the excluded region is mostly determined by the  $\cancel{E}_T$  cut which is effectively fixed by the  $\cancel{E}_T$  trigger threshold. Also shown in Figure 3 are the results from the DØ experiment, based on  $7.4 \text{ pb}^{-1}$ <sup>8</sup>, and from the ALEPH experiment for  $\sqrt{s} = 189 \text{ GeV}$  at LEP<sup>9</sup>.

In the scalar bottom analysis 5 events are selected with an expected background of  $5.8 \pm 1.8$ . The excluded region in  $m_{\tilde{b}_1} - m_{\tilde{\chi}_1^0}$  parameter space is shown in the right plot of Figure 3. The maximum sbottom mass excluded is  $148 \text{ GeV}/c^2$  for  $m_{\tilde{\chi}_1^0} = 0 \text{ GeV}/c^2$ .

DØ combined four channels to set limits on the production of bottom squarks. The first required a  $\cancel{E}_T$  and jets topology. This channel was previously used to set limits on the mass of the top squark<sup>8</sup>. The other three channels in addition required that at least one jet has an associated muon, thereby tagging  $b$  quark decay, and were used to set limits on a charge 1/3 third generation leptoquark for the decay  $LQ \rightarrow \nu_\tau b$ <sup>10</sup>. For all channels, the presence of significant  $\cancel{E}_T$  is used to identify the non-interacting LSP. DØ used identical data samples and event selections as in the stop and third generation leptoquark analyses for the bottom squark limits.

Combining the four channels yields 5 events, with a total estimated background of  $6.0 \pm 1.3$  events. The DØ limits in  $m_{\tilde{\chi}_1^0} - m_{\tilde{b}_1}$  plane are shown in the right plot of Figure 3.

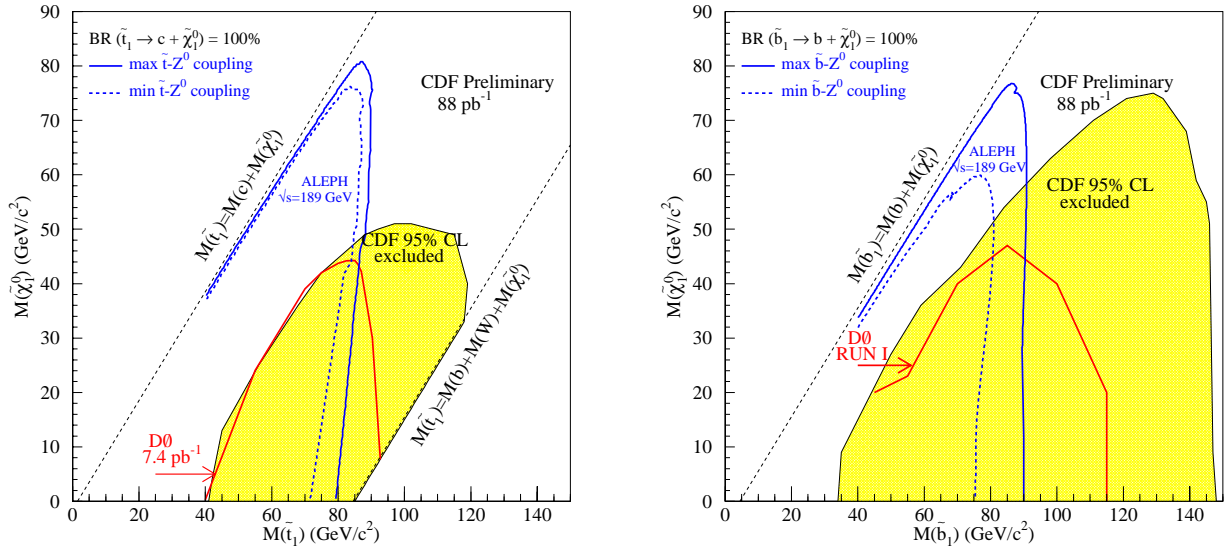


Figure 3: Left plot: 95% CL exclusion region in  $m_{\tilde{\chi}_1^0} - m_{\tilde{t}_1}$  plane for  $\tilde{t}_1 \rightarrow c\tilde{\chi}_1^0$ . Right plot: 95% CL exclusion region in  $m_{\tilde{\chi}_1^0} - m_{\tilde{b}_1}$  plane for  $\tilde{b}_1 \rightarrow b\tilde{\chi}_1^0$ .

### 3 Leptoquark searches

Leptoquarks (LQ) are new particles predicted by many theories of Grand Unification<sup>11</sup>. In these theories LQs mediate transitions between quarks and leptons. The interactions of LQs with lepton and quarks can be described by an effective lagrangian including the most general dimensionless and  $SU(3) \times SU(2) \times U(1)$  invariant couplings<sup>12</sup>. The allowed states are classified according to their spin, weak isospin and fermion number. The couplings are assumed to be baryon- and lepton number conserving in order to avoid rapid proton decay and family diagonal to exclude FCNC beyond CKM mixing. LQs are color triplets and, therefore, are strongly produced at the Tevatron in pairs.

As a particle coupled to two fermions, leptoquark can be a scalar or a vector. In the case of vector LQs the Yang-Mills type couplings may be supplemented by anomalous couplings depending on two parameters  $k$  and  $\lambda$ . They are related to the anomalous 'magnetic' dipole moment and 'electric' quadrupole moment of the LQs in the color field. The production cross section is a strong function of  $k$  and  $\lambda$ . In the following we consider both the cases of purely Yang-Mills type of coupling with  $k=0$  and  $\lambda=0$ , and the minimal vector coupling with  $k=1$  and  $\lambda=0$ . The last one yields considerably smaller cross section compared to Yang-Mills vector LQ.

The phenomenological parameter  $\beta$  determines the decay branching fraction of LQ.  $\beta = 1$  corresponds to a 100% decay branching fraction to a quark and a charged lepton.  $\beta = 0$  corresponds to a 100% decay branching fraction to a quark and a neutrino.

#### 3.1 CDF 2<sup>nd</sup> and 3<sup>rd</sup> generation LQ search

CDF performed a general search for LQs decaying to a heavy quark and a neutrino, i.e. for third generation LQs with charge  $-1/3$  or  $+1/3$  decaying to  $\nu_\tau b$  and the second generation LQs with charge  $+2/3$  or  $-2/3$  decaying to  $\nu_\mu c$ . Both decay modes assume  $\beta = 0$ .

Final states which contain two heavy flavor jets ( $c$ -jets/ $b$ -jets for second/third generations of LQ), large missing energy (from neutrinos), and no high-pt leptons were searched. This is exactly the same signature as in the CDF  $\tilde{t} \rightarrow c + LSP$  and  $\tilde{b} \rightarrow b + LSP$  searches discussed above. The selections and the data sample used for those analyses are optimal for the LQ searches and can be used to set 95% CL cross section limits on the LQ production. The efficiency to the signal ranges from 3% to 7% for

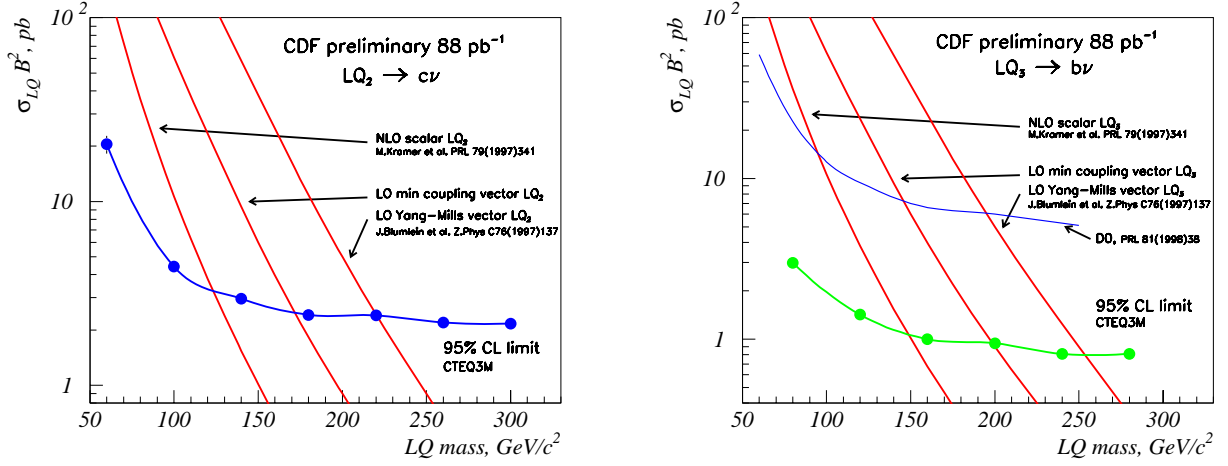


Figure 4: Left plot: CDF 95% CL cross section limits on  $LQ_2 \rightarrow \nu_\mu c$ . Right plot: CDF 95% CL cross section limits on  $LQ_3 \rightarrow \nu_\tau b$ .

the  $\nu_\mu c$  channel and from 6% to 13% for the  $\nu_\tau b$  channel (for  $m_{LQ}$  from 100 to 300  $\text{GeV}/c^2$ ). The efficiencies for vector and scalar LQs are practically the same for the masses above 100  $\text{GeV}/c^2$ .

Figure 4 shows the CDF 95% CL cross section limit on  $LQ_2 \rightarrow \nu_\mu c$  (left plot) and on  $LQ_3 \rightarrow \nu_\tau b$  (right plot) together with the expected theoretical cross sections for scalar and two types of vector LQs. The scalar  $LQ_2$  with mass less than 122  $\text{GeV}/c^2$  and  $LQ_3$  with mass less than 149  $\text{GeV}/c^2$  are excluded by this analysis.

### 3.2 $D\bar{O}$ 2<sup>nd</sup> generation LQ search

$D\bar{O}$  performed a new search for the second generation LQ in the  $\mu\mu jj$  and  $\mu\nu jj$  channels. The first channel has the best sensitivity for  $\beta = 1$ , while the second channel is more sensitive for  $\beta = 0.5$ . The results are based on neural network analyses and use 94  $\text{pb}^{-1}$  of data. The dimuon analysis requires events to contain two muons with  $p_T^{\mu_{1,2}} > 20$   $\text{GeV}/c$  and two jets with  $E_T^{j_{1,2}} > 20$   $\text{GeV}$ . In addition, events must satisfy an event topology cut. The data sample contains 52 events with  $53 \pm 13$  events expected from background (primarily from  $W/Z + jets$ ,  $WW$ , and  $t\bar{t}$  production). Seven kinematic quantities are used as input to the neural network:  $E_T^{j_1}, E_T^{j_2}, p_T^{\mu_1}, p_T^{\mu_2}, E_T^{j_1} + E_T^{j_2}, (E_T^{j_1} + E_T^{j_2}) / \sum E_T^{j_i}$ , and  $m_{\text{event}}$  where  $m_{\text{event}}$  is the invariant mass of the muons and jets. The left plot in Figure 5 shows the neural network discriminant distribution for the data, background and signal events.

After applying a final selection on the output of the neural network, the estimated background is  $0.7 \pm 0.3$  events; no events remain in the data sample. The signal efficiency ranges from 10% to 25% for leptoquark masses between 140 and 400  $\text{GeV}/c^2$ .

The right plot in Figure 5 shows 95% CL cross section limits on  $LQ_2 \rightarrow \mu q$  for  $\beta = 1$  and  $\beta = 0.5$ .

The single muon analysis requires events containing one muon with  $p_T^\mu > 25$   $\text{GeV}/c$ , two jets with  $E_T^{j_{1,2}} > 15$   $\text{GeV}$ , and  $\cancel{E}_T > 30$   $\text{GeV}$ . In leptoquark events, the muon and neutrino are uncorrelated since they come from different particles, unlike the muon and neutrino in  $W + jets$  events. To reduce this background, the muon and  $\cancel{E}_T$  must be well separated in azimuth and the two jets must be well separated in  $\eta - \phi$  space. After this selection,  $108 \pm 30$  events are expected from SM backgrounds and 109 events remain in the data sample. A smaller neural network is used here, with four kinematic quantities as inputs:  $p_T^\mu, E_T^{j_1}, E_T^{j_2}$ , and  $\cancel{E}_T$ . After cutting on the neural network output, no events remain in the data, with an expected background of  $0.7 \pm 0.9$  events. The efficiency for identifying leptoquarks is 4% for  $M_{LQ_2} = 100$   $\text{GeV}/c^2$  and 17% for  $M_{LQ_2} = 400$   $\text{GeV}/c^2$ .

The two channels  $\mu\mu jj$  and  $\mu\nu jj$  have been combined to exclude the second generation scalar leptoquarks with mass less than 200  $\text{GeV}/c^2$  for  $\beta = 1$  and less than 180  $\text{GeV}/c^2$  for  $\beta = 0.5$ .

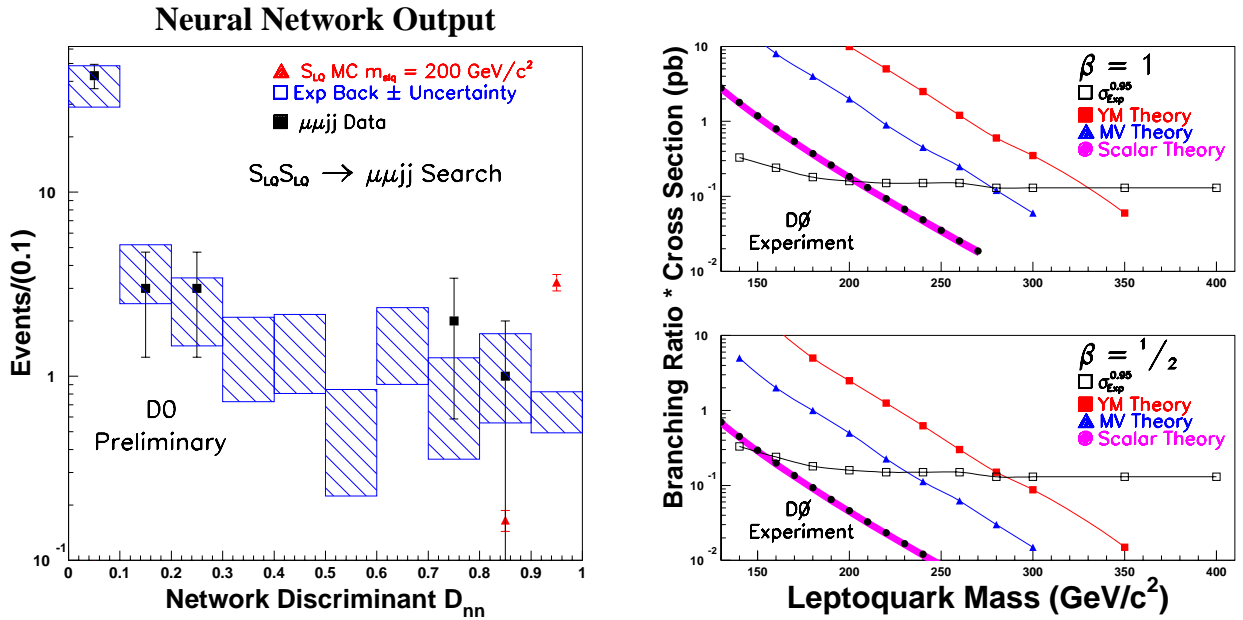


Figure 5:  $\mu\mu jj$  channel. Left plot: Neural network output for the data, background and signal events. Right plot: DØ 95% CL cross section limits on  $LQ_2 \rightarrow \mu q$ .

## Conclusion

Searches for supersymmetric and leptoquark signatures at the Tevatron are consistent with SM expectations. As a result a significant area of the parameter space of various SUSY models and leptoquark masses has been excluded.

The CDF and DØ collaborations are looking forward for Run II with the Main Injector and the upgraded detectors. Most of Tevatron searches are limited by the luminosity and a factor of 20 increase in the luminosity in Run II will allow us to probe deeper various models and to possibly discover new phenomena.

## Acknowledgments

We thank the Fermilab staff and the technical staffs of the participating institutions for their vital contributions. This work was supported by the U.S. Department of Energy and National Science Foundation; the Istituto Nazionale di Fisica Nucleare (Italy); the Ministry of Education, Science and Culture (Japan); the Natural Sciences and Engineering Research Council (Canada); the National Science Council (China); the A. P. Sloan Foundation; the Swiss National Science Foundation; the Commissariat a L'Energie (France); the State Committee for Science and Technology and Ministry for Atomic Energy (Russia); CAPES and CNPq (Brasil); the Department of Atomic Energy and Science and Education (India); Colciencias (Colombia); CONACyT (Mexico); the Ministry of Education and KOSEF (Korea); and CONICET and UBACyT (Argentina).

## References

1. S. Abachi et al. [DØ collaboration], Nucl. Instr. Meth. **A338**, 185 (1994).
2. F. Abe *et al.* [CDF Collaboration], Nucl. Instr. Meth. **A271**, 387 (1988).
3. For review of SM see for ex. L. Susskind, *Phys. Rev. D* **20**, 2619 (1979).

4. For reviews of SUSY see H. P. Niles, *Phys. Rev. D* **110**, 1 (1984);  
H. E. Haber and G. L. Kane, *Phys. Rev. D* **117**, 75 (1985).
5. P. Fayet, *Phys. Lett.* **B70**, 461 (1977) and *Phys. Lett.* **B86**, 272 (1979).  
J. Ellis, K. Enqvist and D. Nanopoulos, *Phys. Lett.* **B147**, 99 (1984).
6. A. Brignole, F. Feruglio, M.L. Mangano and F. Zwirner, *Nucl. Phys.* **B526**, 136 (1998).
7. H. Baer *et al.*, *Phys. Rev.* **D44**, 725 (1991).  
H. Baer, J. Sender and X. Tata, *Phys. Rev.* **D50**, 4517 (1994)
8. S. Abachi *et al.* [D0 Collaboration], *Phys. Rev. Lett.* **76**, 2222 (1996).
9. R. Barate *et al.* [ALEPH Collaboration], "Searches for sleptons and squarks in e+e- collisions at  $\sqrt{s}=188.6$  GeV" submitted to *Phys. Lett. B*
10. B. Abbott *et al.* [D0 Collaboration], *Phys. Rev. Lett.* **81**, 38 (1998).
11. see for example, J.C.Pati and A.Salam, *Phys. Rev. D* **8**, 1240 (1973);  
J.C.Pati and A.Salam, *Phys. Rev. Lett.* **31**, 661 (1973);  
J.C.Pati and A.Salam, *Phys. Rev. D* **10**, 275 (1973);  
H.Georgi and S.L.Glashow, *Phys. Rev. Lett.* **32**, 438 (1974);  
B.Schrempp and F.Schrempp, *Phys. Rev. Lett.* **B153**, 101 (1985);
12. W.Buchmüller, R.Ruckl and D.Wyler *et al.*, *Phys. Rev. Lett.* **B191**, 3 (1987)